Systematic Entomology

Systematic Entomology (2021), **46**, 672–684 DOI: 10.1111/syen.12482

X-ray microtomography and phylogenomics provide insights into the morphology and evolution of an enigmatic Mesozoic insect larva

DAVIDE BADANO[1,2], MICHELA FRATINI[3,4], LAURA MAUGERI[3,4], FRANCESCA PALERMO[3,5], NICOLA PIERONI[3,6], ALESSIA CEDOLA[3], JOACHIM T. HAUG[7,8], THOMAS WEITERSCHAN[9], JÜRGEN VELTEN[10], MAURIZIO MEI[1,2], ANDREA DI GIULIO[11,12] and PIERFILIPPO CERRETTI[1,2,13]

[1]Department of Biology and Biotechnologies "Charles Darwin", Sapienza University of Rome, Rome, Italy, [2]Museum of Zoology, Sapienza University of Rome, Rome, Italy, [3]CNR-Nanotec (Rome unit) c/o Department of Physics, Sapienza University of Rome, Rome, Italy, [4]IRCCS Santa Lucia Foundation, Rome, Italy, [5]Department of Morphogenesis Tissue Homeostasis, Sapienza University of Rome, Rome, Italy, [6]Department of Physics, University of Calabria, Arcavacata di Rende, Italy, [7]Ludwig-Maximilians-Universität München, Biocenter, Munich, Germany, [8]GeoBio-Center of the LMU Munich, Munich, Germany, [9] Höchst im Odenwald, Germany, [10] Kirchheimbolanden, Germany, [11]Department of Science, University Roma Tre, Rome, Italy, [12]Interdepartmental Laboratory of Electronic Microscopy (LIME), University Roma Tre, Rome, Italy and [13]Australian National Insect Collection, CSIRO National Facilities and Collections, Canberra, Australia

Abstract. Fossils sometimes show unusual morphological features absent in living organisms, making it difficult to reconstruct both their affinity and their function. We describe here a new lacewing larva, *Ankyloleon caudatus* **gen. et sp.n.** (Neuroptera) from the Cretaceous amber of Myanmar, characterized by an abdomen unique among insects, with 'tail-like' terminal segments bearing a ventral pair of vesicles. Phase-contrast X-ray microtomography reveals that these structures were dense and equipped with a median duct, suggesting that they were likely pygopods used for locomotion, holding the position through adhesive secretions. Our phylogenetic analyses, combining genomic and morphological data from both living and fossil lacewings, proved critical to placing *Ankyloleon* **gen.n.** on the lacewing tree of life as an early representative of the antlion clade, Myrmeleontiformia. These results corroborate the view that derived myrmeleontiform lacewings 'experimented' with unusual combinations of features and specializations during their evolutionary history, some of which are now lost.

Zoobank registration: urn:lsid:zoobank.org:pub:0C0AC565-1AC9-42CC-831D-EDA38BA36F64

Introduction

There is general agreement among scientists that winged insects (Pterygota) spawned the most spectacular radiation of metazoans on Earth (Misof *et al.*, 2014; Haug J.T. *et al.*, 2015). So far, more than one million extant pterygotes have been described, and the fossil record provides evidence that these organisms played a key role in virtually all terrestrial ecosystems since the late Paleozoic (Grimaldi & Engel, 2005; Labandeira, 2018). Pterygote diversity is heavily skewed phylogenetically towards Holometabola (wasps, bees, ants, beetles, moths, butterflies, flies), which roughly comprise 90% of their diversity (Grimaldi & Engel, 2005; Peters *et al.*, 2014). Recent phylogenomic reconstructions of insects suggest that Holometabola differentiated relatively early, during the Devonian (Misof *et al.*, 2014; Peters *et al.*, 2014; Montagna *et al.*, 2019), although the first fossils (including

Correspondence: Davide Badano and Pierfilippo Cerretti, Department of Biology and Biotechnologies "Charles Darwin", Sapienza University of Rome, Piazzale A. Moro 5, 00185 Rome, Italy. E-mail: davide.badano@uniroma1.it (D. B.), E-mail: pierfilippo.cerretti@uniroma1.it (P. C.)

larvae) are more recent, dating back to the Moscovian stage (Carboniferous 315–303 Ma) (Nel *et al.*, 2013; Haug J.T. *et al.*, 2015). Holometabolans evolved a modular separation between postembryonic developmental (larva) and reproductive (adult) stages through a dramatic change of larval anatomy that takes place during an intermediate pupal stage. The evolution of this strategy exposed larvae and adults to different selective pressures, allowing a differential, temporal and compartmentalized exploitation of resources and thus eliminating intraspecific competition between life stages (Truman & Riddiford, 1999; Yang, 2001; Beutel *et al*., 2014; Rainford *et al.*, 2014; Rolff *et al.*, 2019; Truman, 2019). Larvae evolved into voracious feeders as their body developed to store the energy needed for metamorphosis and an adult life. In particular, the abdomen – the tagma most involved in energy storage – increased in size and weight, often becoming involved in locomotion unlike that of adults. To our knowledge, such a novel function of the larval abdomen has never been exploited by nonholometabolans, nor by any nonpaedomorphic, adult pterygotes.

Neuroptera (lacewings) are a monophyletic group of holometabolans displaying marked disparity in larval life strategies and morphology, despite their relatively poor extant species diversity (ca. 6000 described species) (Engel *et al.*, 2018; Oswald & Machado, 2018). Neuroptera, together with the allied groups Raphidioptera (snakeflies) and Megaloptera (alderflies and dobsonflies), form the clade Neuropterida, which represents the sister group to Coleopteroidea (Strepsiptera and Coleoptera) (Winterton *et al.*, 2018; Vasilikopoulos *et al.*, 2020). The Cretaceous witnessed an explosive phase of evolutionary experimentation in lacewings. In that period, now-extinct larval phenotypes coexisted with forms that were almost identical to those living today, already displaying complex behaviours like camouflaging and mimesis (Pérez de la Fuente *et al.*, 2012, 2016, 2018a, b, 2020; Liu *et al.*, 2016, 2018; Wang *et al.*, 2016; Badano *et al.*, 2018; Haug J.T. *et al.*, 2018, Haug C. *et al.*, 2019, Haug J.T. *et al.*, 2019a, 2019b; Haug G.T. *et al.*, 2020; Haug J.T. *et al.*, 2020). Lacewing larvae and adults appear especially diverse and abundant in the Late Cretaceous 'Burmese' amber from Myanmar (ca. 99 million years) hinting at a possible prominent ecological role of this group at that time (Wang *et al.*, 2016; Badano *et al.*, 2018; Lu & Liu, 2021). Recent findings have shown that much of now-extinct lacewing morphologies are likely yet to be discovered and, indeed, the full depth of their evolutionary experimentation is not yet understood. Here, we describe a novel larval body organization from the Myanmar amber deposit, which, to our knowledge, has no analogue among living insects. Examined specimens, although sharing all the autapomorphic features that support the monophyly of Neuroptera, such as the modification of mandible and maxilla in a sucking apparatus and lack of maxillary palp (Beutel *et al.*, 2010), drastically depart from the typical organization of lacewing larvae by having the second half of the abdomen abruptly narrowing, elongated and ending in a spatula-like structure equipped with relatively large ventral vesicles. Overall, the abdomen is reminiscent of the division in meso- and metasoma characterizing scorpions, although in this case the function is completely unknown. These modifications are not only unique throughout all known fossil and living insects but also among all hexapods, suggesting highly specialized habits. We examined the morphology of this fossil through synchrotron X-ray phase-contrast microtomography (XPCT) to explore in detail fine, internal anatomical features and hypothesize which selective forces likely shaped this extreme shape within the broader context of lacewing evolution. XPCT is a nondestructive 3D imaging technique endowed with higher image contrast and spatial resolution than conventional tomography, which also detects minor electronic density variations due to sensitivity to phase shift. This technique appears particularly helpful when applied to fossils, yielding detailed information, especially if combined with conventional micro-CT (Tafforeau *et al.*, 2006; Lak *et al.*, 2008; Soriano *et al.*, 2010; Perreau & Tafforeau, 2011; Bidola *et al.*, 2015). Moreover, we tested the affinities of fossil larvae with living species by combining morphological and molecular data. Our findings suggest that (i) complex anatomical structures evolved as dead-end innovations during a phase of morphological diversification and (ii) the integration of genomic data with morphological information allows for the determination of the affinities of enigmatic stem-group phenotypes.

Materials and Methods

Origin of specimens and depository

The examined fossil materials were extracted from the amber outcrops of northern Myanmar, located in Kachin Province, ca. 100 km west of the town of Myitkyina. These deposits are dated at the very beginning of the Late Cretaceous near the Aptian/Cenomanian border (Shi *et al.*, 2012). However, the discovery of other outcrops in the region, dating back from the same stage but slightly younger (Zheng *et al.*, 2018), makes it difficult to pinpoint with certainty the fossil provenance. As far as the authors can ascertain, the amber pieces were obtained legally and before the upheaval and humanitarian crisis in the area. The holotype of *Ankyloleon caudatus* **sp.n.** (MZURPAL00111) and *Ankyloleon* specimen 1 (MZURPAL00112) are deposited in the public collection of the Zoological Museum of Sapienza University of Rome, Italy; *Ankyloleon* specimen 2 (BUB3) is deposited in T. Weiterschan private collection, Höchst Odw., Germany; *Ankyloleon* specimen 3 (PED_0118) and *Ankyloleon* specimen 4 (PED_0454) are deposited in the public collection of the Ludwig-Maximilians-Universität, Munich, Germany.

Morphological abbreviations

The following abbreviations are used in the caption of the figures: 7 = abdominal segment 7; 8 = abdominal segment 8; 9 = abdominal segment 9; 10 = abdominal segment 10; abd = abdomen; ant = antenna; dct = duct; hc = head capsule; hd = head; md = mandible; ms = mesonotum; mt = metanotum; mx = maxilla; ne = neck region; ot = ocular tubercle; pr = pore; prn = pronotum; pyg = pygopods; rst = rastra; S5 = sternite 5; S6 = sternite 6; S7 = sternite 7; S8 = sternite 8; S9 = sternite 9; S10 = sternite 10; sp = spiracle; thr = thorax; trc = tracheae.

Imaging

Specimens were examined and measured with a Leica© (Wetzlar, Germany) MZ 9.5 stereomicroscope equipped with an ocular micrometre. Photos were taken with a Canon© (Tokyo, Japan) EOS 600D digital camera with Canon© lens MP-E 65 mm. The resulting images were focus-stacked with the software Zerene© (Richland, WA, U.S.A.).

X-ray phase-contrast microtomography

The experiments were carried out at the TOMCAT beamline of the Swiss Light Source (Villigen, Switzerland). The incident monochromatic X-ray energy was of 20 keV. A PCO edge 5.5 camera coupled with optics resulting in a pixel size of $1.625 \times 1.625\,\mu m^2$ and $0.32 \times 0.32\,\mu m^2$ was set at a distance from the sample of 3 and 5 cm, respectively. The tomographic images were acquired with an exposure time of 90 ms for $1.625 \times 1.625\,\mu m^2$ and exposure time of 220 ms for $0.32 \times 0.32\,\mu m^2$ covering a total angle range of 360°, using the so-called half-acquisition mode, which allows to almost double the image field of view. Then, the tomographic projections were reconstructed *on site* by means of ad hoc software based on the Paganin's phase retrieval algorithm. Image processing and 3D rendering were made with the software ImageJ (https://imagej.net/Fiji) and 3D slicer (https://www.slicer.org/) and Amira.

Scanning electron microscopy

Extant lacewing larvae preserved in 70% ethanol were dehydrated in a graded ethanol series to 100% ethanol, critical point dried in a CPD 030 unit (BalTec©, Balzers, Liechtenstein) and secured to aluminium stubs using conductive double adhesive carbon discs. Subsequently, the samples were sputter-coated with a thin layer (30 nm) of gold, using a K550 sputter coater (Emithech©, Kent, UK) and examined with a Zeiss© Gemini Sigma 300 (Jena, Germany) field-emission scanning electron microscope, with an Everhart-Thornley© secondary electron detector and an acceleration tension of 5 kV, in the Laboratorio Interdipartimentale di Microscopia Elettronica, Roma Tre University, Rome, Italy.

Phylogenetic analyses

The genomic dataset is an excerpt of the nucleotide alignment of Winterton *et al.* (2018) including 57 taxa – i.e., pruned of those with unavailable information on larval morphology – and 57546 bp. The morphological datasets were assembled in Mesquite integrating recently published matrices (Beutel *et al.*, 2010; Badano *et al.*, 2017; Jandausch *et al.*, 2019) for extant species and (Badano *et al.*, 2018) for fossils. The two morphological matrices included 137 characters and are identical except in the number of taxa. The matrix of extant species included 57 taxa, whereas the set encompassing fossils comprised 76 taxa. When information about larval morphology was not available for terminal taxa, morphological characters were scored from congeners.

The partitioned maximum likelihood (ML) analyses, combining the genomic and the molecular datasets, were performed in IQ-TREE (v.2.1.1) (Minh *et al.*, 2020) on Extreme Science and Engineering Discovery Environment (XSEDE) at Cyberinfrastructure for Phylogenetic Research (CIPRES) (Miller et al., 2010). Models were computed separately for the two datasets as different partitions, enforcing the Model Finder option implemented in IQ-TREE (Chernomor *et al.*, 2016; Kalyaanamoorthy *et al.*, 2017). The mixed partitions had different speeds and applied 50 independent tree searches. Node supports were estimated using ultrafast bootstrap (Hoang *et al.*, 2018) performing 10 000 replicates (Fig. S4).

The Evolutionary Placement Algorithm (EPA) was developed (Berger & Stamatakis, 2010) and implemented in RAxML (Stamatakis, 2014). EPA integrates molecular and morphological datasets, placing taxa for which only morphological data are available in a molecular tree in a two-step process. We ran all the analyses using RAxML-HPC2, version 8, on the XSEDE at CIPRES Science Gateway (Miller *et al.*, 2010). First, we generated a phylogenomic tree enforcing a GTR+I+Γ substitution model and included a rapid bootstrap search of 100 replicates starting at a random seed number. Then, we supplied the obtained molecular tree and the morphological dataset of extant taxa to calibrate weights for each morphological character, based on congruence between the molecular and morphological inputs. In the following step, we provided a morphological dataset inclusive of fossils, allowing EPA to estimate the likelihoods of fossil placement in the genomic tree through the morphological weights (Fig. S5).

Maximum parsimony analyses of the morphological dataset were performed with TNT, version 1.5 (Goloboff & Catalano, 2016), with the "traditional search option" enforcing the following settings: general RAM of 1 GB, memory set to hold 1 000 000 trees, setting 1000 replicates with tree bisection reconnection and saving 1000 trees per replicate; multistate characters were treated as unordered. Character state changes (apomorphies) were optimized in WinClada, version 1.00.08 (Nixon, 2002) (Figs S6, S7).

Results

Taxonomy

Ankyloleon Badano, Haug & Cerretti **gen.n.**

Zoobank registration: lsid:zoobank.org:act:DB189598-97C1-4684-AE3A-0548CCD80F03

Etymology. The generic epithet is a masculine name from Greek, composed of a prefix referring to the dinosaur genus *Ankylosaurus* Brown (Ornithischia, Ankylosauridae) based on the shape of abdominal segment 10 of the larva, which resembles the caudal club of the famous dinosaur, but also on *ankylos* 'bent, crooked' after the apical bending of jaws; the Greek suffix *-leon* means 'lion' and is commonly used in antlion genera.

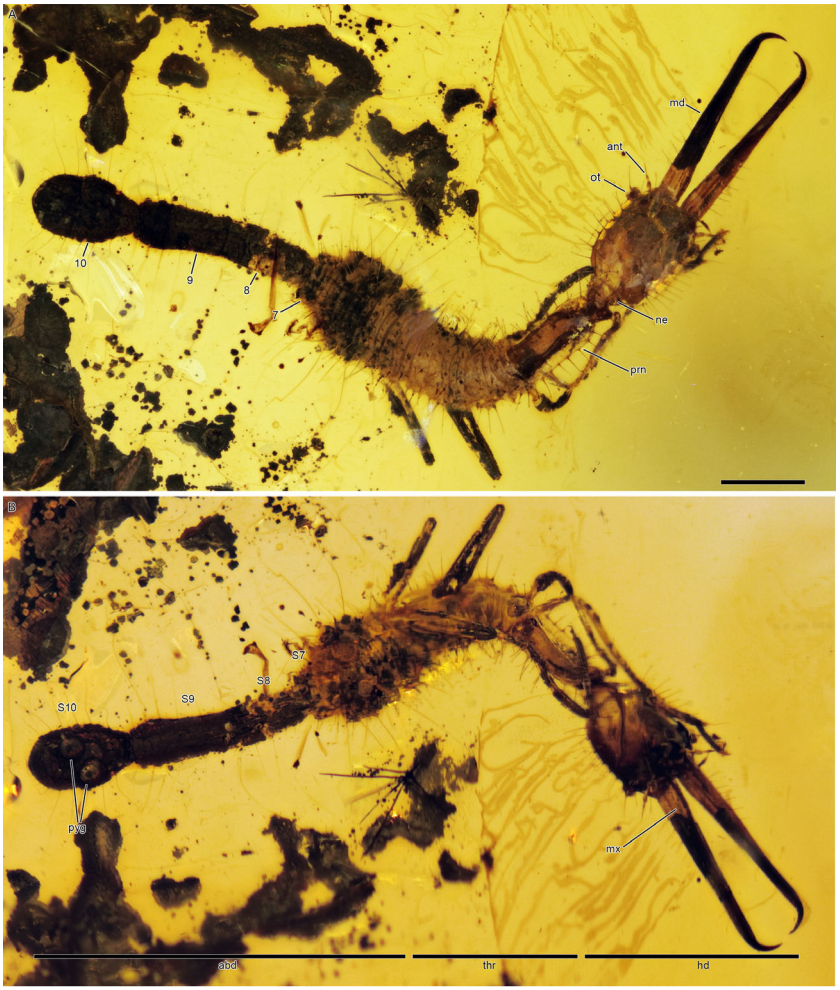

Fig. 1. *Ankyloleon caudatus* **gen. et sp.n.** holotype (MZURPAL00111): (A) dorsal view and (B) ventral view. Scale bar: 500 µm. [Colour figure can be viewed at wileyonlinelibrary.com].

Diagnosis. Campodeiform, elongate lacewing larva; head capsule sclerotized; stemmata on distinct tubercle; antenna short and three segmented; mandibular–maxillary stylets elongate, straight, curved inwards only at apex, without teeth; prothorax elongated, tubular; abdomen subdivided in an anterior section with six short segments and a posterior narrower section (Figs 1, 2).

Type species. Ankyloleon caudatus **sp.n.**

Ankyloleon caudatus Badano, Haug & Cerretti **sp.n.**

Zoobank registration: urn:lsid:zoobank.org:act:0EE58540-1521-4DB3-A8E9-FAF44F4D22D7

Holotype. MZURPAL00111 (Museum of Zoology, Sapienza University of Rome). One specimen preserved in an amber piece; state of preservation good; complete (Fig. 1).

Locality and Horizon. Northern Myanmar (see Section 2), Late Cretaceous (Cenomanian).

Etymology. The specific name is an adjective derived from the Latin *cauda* and meaning 'tailed', after the tail-like section of abdomen.

Description. Body length 3.28 mm. Head capsule longer (length 0.58 mm) than wide (width 0.44 mm), globose in lateral view but tapering anteriorly; ventral surface flat (Fig 1A, B). Ocular region raised on tubercle, bearing six stemmata (five dorsal, one ventral) and with apical trichoid sensillum, twice as long as tubercle height and borne on elevated base (Fig. 1A). Antenna short, 1/5 the length of mandible, tapering apically (Fig. 1A). Jaws (mandibular–maxillary stylets) two times longer than head capsule (mandible length 0.96 mm), straight, curved inwards at apex, almost in contact at insertion; mandible wider at base, internal margin with minute serrations, without teeth, external margin with long trichoid sensilla (Fig. 1A, B). Labial palp absent. Posterior section of head progressively tapering in a neck-like region (Fig. 1A). Dorsal side of head with long trichoid sensilla orderly arranged in rows and raised from circular alveoli. Cervix short, apparently membranous.

Prothorax cylindrical, elongate, two times longer than wide (Fig. 1A, B). Pronotum sclerotized, tubular, covered with trichoid sensilla (Fig. 1A). Meso- and metanotum entirely membranous, thickly covered by setae. Setiferous tubercles absent.

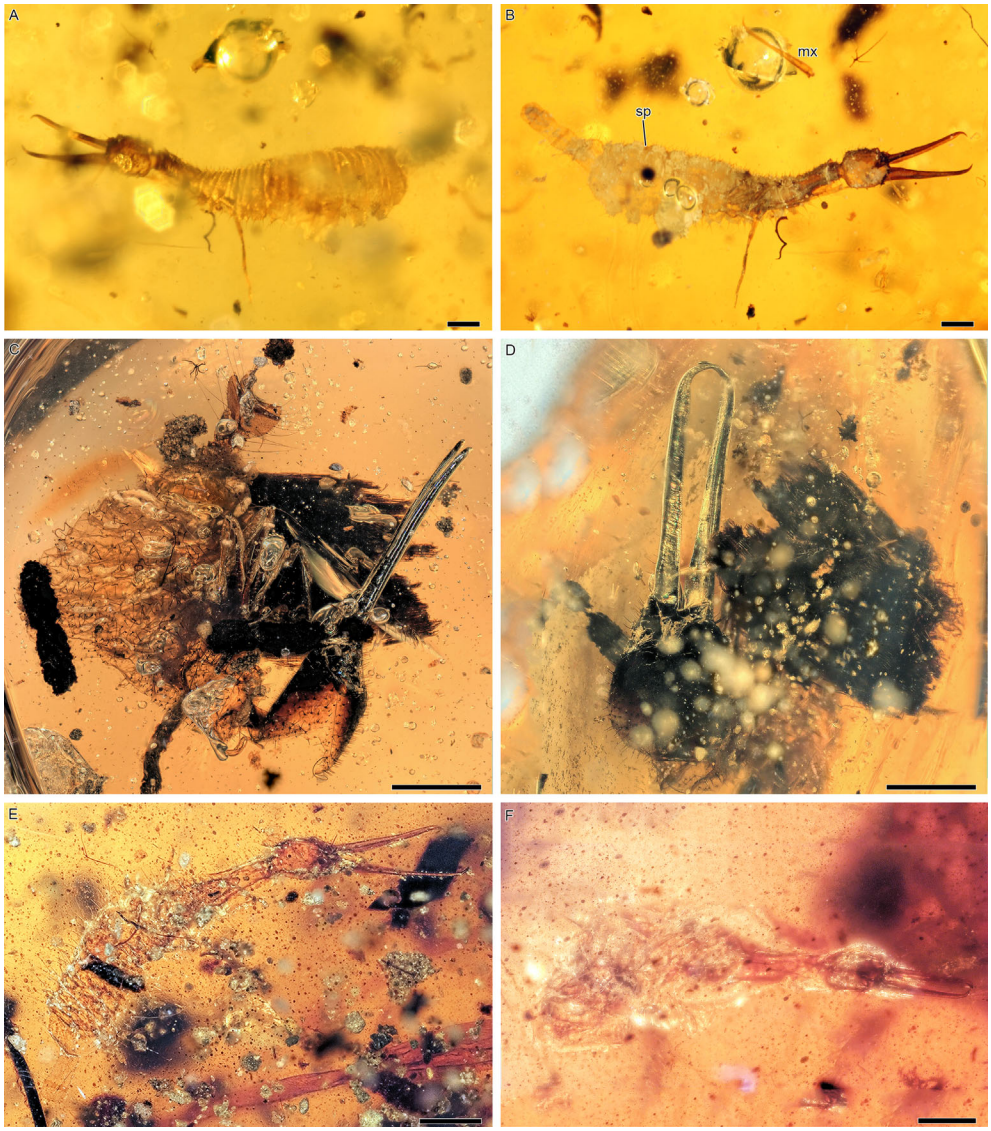

Fig. 2. Other specimens of *Ankyloleon*. (A, B) *Ankyloleon* specimen 1, (MZURPAL00112): (A) dorsal view, (B) ventral view, (C, D) *Ankyloleon* specimen 2 (BuB 3), (E) *Ankyloleon* specimen 3 (PED_0118) and (F) *Ankyloleon* specimen 4 (PED_0454). Scale bar: 500 μm. [Colour figure can be viewed at wileyonlinelibrary.com].

Leg pairs of similar length and shape, relatively long and slender; femora as long as tibiae; tarsi elongate, not subdivided; pretarsal claws small and hook-shaped, empodium absent (Fig. 1B).

Abdominal segments 1–6 not differentiated from thorax, relatively broad, not sclerotized and covered with long setae (Fig. 1A, B). Segment 7 as a short truncate cone. Segments 8–10 strongly modified into a narrow, elongate caudal section almost as long as the rest of the body. Segment 8 cylindrical, two times longer than wide. Segment 10 spatula-shaped, proximally invaginated within the cuticle of segment 9 (Figs 1A, B, 3B). Ventral side of segment 10 with a pair of prominent, symmetrical vesicle-like structures with a central pore prolonged internally into a tube-like channel (Fig. 1B, 3C). Segments 8–10 covered with thin hair-like setae, longer on body outline; terminal "spatula" with long thin sensilla along lateral margin (Fig. 1A, B).

Other Ankyloleon *specimens* (File S1). Materials. *Ankyloleon* specimen 1, MZURPAL00112 (Museum of Zoology, Sapienza University of Rome). *Ankyloleon* specimen 2, Nr. BuB 3 (T. Weiterschan Coll.); *Ankyloleon* specimen 3, PED_0118 (LMU Munich) (Fig. S2); *Ankyloleon* specimen 4, PED_0454 (LMU Munich) (Fig. S3).

Comments. These four fossil larvae can be assigned to *Ankyloleon*, though their state of preservation or completeness does not allow for the study of several key morphological features (Figs 2, S1, S2, S3). Thus, it is not possible to fully compare them with *A. caudatus* **sp.n.**, only allowing us to place them to genus. However, these specimens share the apomorphic

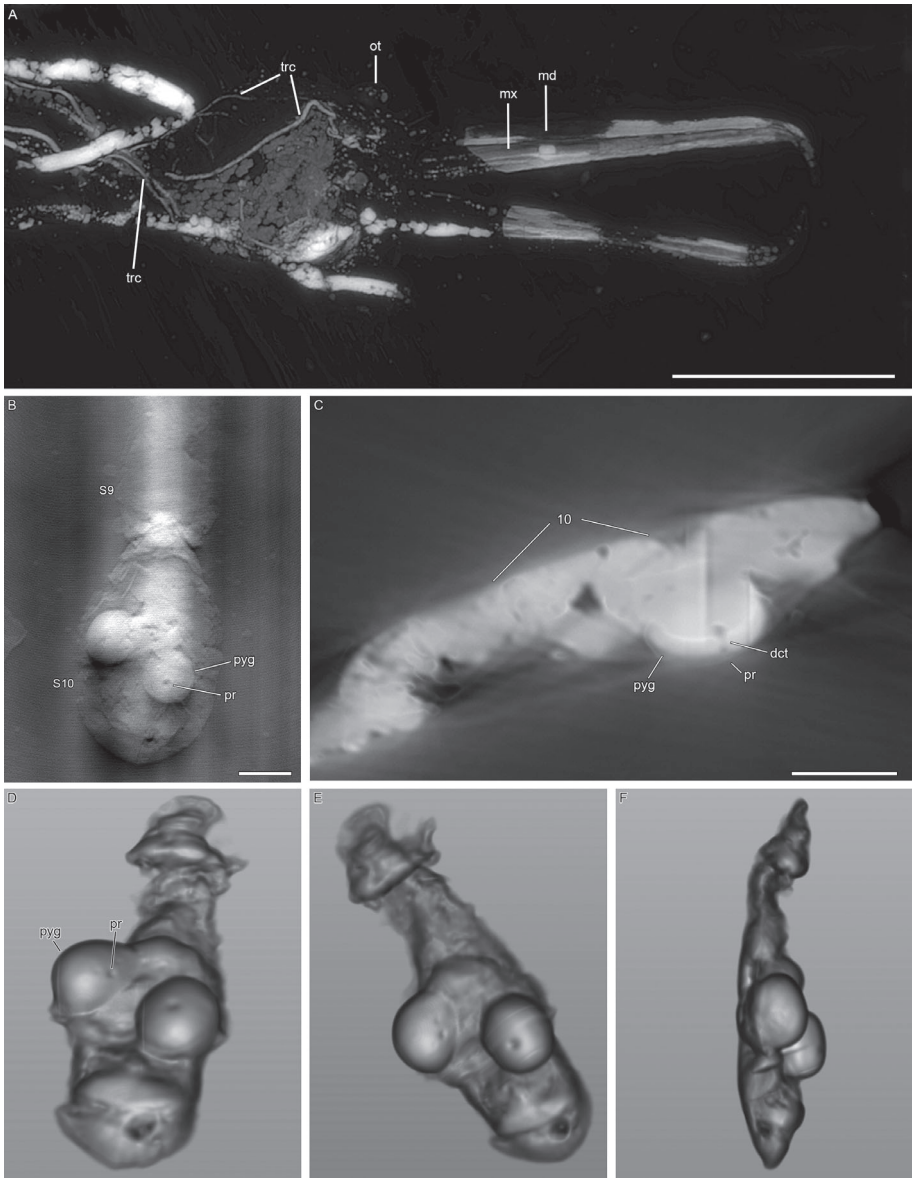

Fig. 3. X-ray phase-contrast microtomography scan of *Ankyloleon caudatus* **gen. et sp.n.** holotype: (A) head and mouthparts, ventral view, scale bar: 500 µm; (B) Abdominal segment 10 and pygopods, ventral view, scale bar: 100 µm; (C) abdominal segment 10 and pygopods, cross section, scale bar: 30 µm, (D–F) 3D reconstruction of abdominal segment 10 and pygopods; (D, E) ventral view and (F) lateral view.

characteristics of *Ankyloleon* such as long jaws only bent at apex, antenna short, tubular pronotum and abdominal segments 9 and 10 differentiated from the rest of the abdomen as a narrow posterior section. These larvae are characterized by shorter, less differentiated segments 9–10 with respect to *A. caudatus* and by the absence of a distinct spatula. Among them, the best-preserved specimen, that is, *Ankyloleon* specimen 1, is also provided with paired sclerotized pygopods on abdominal segment 10, demonstrating that this character was not exclusive of *A. caudatus* nor a fossilization artefact (Fig. S1). However, this specimen differs from *A. caudatus* in chaetotaxy, as the setae covering the body are relatively short and stout (hair-like in *A. caudatus*) (Fig. 2; File S1). The similar size of the specimens suggests that these differences were not ontogenetic, so these larvae likely belonged to different species.

Morphological remarks. Ankyloleon shares the following combination of character states with Myrmeleontiformia: (i) ocular tubercles, (ii) temple region, (iii) neck region, (iv) posterior tentorial grooves on the anterior portion of the head capsule, (v) maxilla half the size of mandible (Badano *et al*., 2018), but lack of dolichasterine setae. Interestingly, maximum parsimony analysis of the morphological dataset reconstructed *Ankyloleon* within Myrmeleontiformia (Figs S6, S7) based on a series of inferred character state changes (59:1, premental elements

widely separated; 68:1, gular region with a small anterior triangular sclerite; 69:1, hypostomal bridge present; 72:2, posterior tentorial grooves on anterior portion of head capsule), which are not observable in our specimens, due to bad state of preservation or amber impurities (Figs 1, 2). The jaws of *Ankyloleon* recall those of Nevrorthidae, but its head capsule is greatly different. *Ankyloleon* lacks labial palpus like the larvae of spongillaflies (Sisyridae), and the long sensilla on its head resemble those of mantispoid larvae (Berothidae, Rhachiberothidae, Mantispidae). This combination of features, along with its outstanding autapomorphic abdominal shape, makes this taxon not readily assignable to any recognized family-ranked group. The homology assessment of the abdominal segmentation in *Ankyloleon* was determined by comparing *A. caudatus* with the other larvae through the arrangement of the abdominal spiracles (File S1). Boundaries of abdominal segments are difficult to identify in larvae of Myrmeleontiformia as their cuticle is soft, wrinkled and almost annulate, lacking tergal and sternal sclerites. Immature Myrmeleontiformia have a pair of spiracles on abdominal segments 1–8. *Ankyloleon* instead bears one pair of spiracles only on abdominal segments 1–6; this is likely a consequence of the great morphological changes segments 7 and 8 have undergone. There are no morphological cues help determine at which instar the examined larvae of *Ankyloleon* belong. Interestingly however, *Ankyloleon* specimen 3 is an exuvia, which means that it could more likely represent a first or second instar because third (last) instars encase themselves in a silky cocoon before pupation and leave their exuvial remains within it.

Phase-contrast XPCT

XPCT images (Fig. 3, Movie S1, Movie S2) show that the state of preservation of the cuticle of the anterior portion of the holotype, including head, part of jaws, thorax and appendages did not provide enough contrast to reconstruct an accurate 3D outline. The tracheal respiratory system is rendered in some detail, showing the longitudinal branches of the anterior tracheal system extending from thorax to head (Fig. 3A). Abdominal segment 10 is rendered as a wide, relatively thick, dorsoventrally depressed, structure; it is roughly drop-shaped in dorsal view, narrowing at the insertion with segment 9 (Fig. 3B, D, E). The paired ventral vesicles are dense, thick, ovoid structures, clearly emerging from the body outline in lateral view (Fig. 3B–D). The XPCT cross- sections of vesicles show a perpendicular duct (Fig. 3C), which is externally visible as a median pore (Fig. 3B–E).

Phylogenetic analysis

We explored the phylogenetic placement of *Ankyloleon* and a selection of larvae of key extinct taxa on the lacewing tree of life, using two maximum likelihood-based optimizations (ML): (i) running a combined (or total evidence) phylogenetic analysis of genomic and morphological data (Figs 4, S4) and (ii) employing the EPA on a ML tree obtained with genomic data only (Berger & Stamatakis, 2010; Berger *et al.*, 2011) (Figs 4, S5). Both approaches yielded trees that were largely consistent with that of Winterton *et al.* (2018) and largely agreed on the placement of fossil taxa (Fig. 4). Cretaceous taxa *Pedanoptera* Liu *et al.* and *Hallucinochrysa* Pérez de la Fuente *et al.* were recovered as sister to all extant chrysopids in the combined analysis. EPA instead recovered *Hallucinochrysa* as a crown-group Chrysopidae. *Macleodiella* Badano & Engel was consistently reconstructed sister to all the remaining Myrmeleontiformia. The position of *Ankyloleon* changed depending on the analysis but its affinities with Myrmeleontiformia were well supported under both methods (see also Figs S6, S7). The combined ML analysis recovered *Ankyloleon* nested within Myrmeleontiformia, as a member of the monophyletic group including Nymphidae (split-footed lacewings) and Ithonidae (moth lacewings) (Fig. 4). EPA instead found *Ankyloleon* as sister to Myrmeleontiformia, except *Macleodiella* (Fig. 4). Both analyses consistently placed *Aphthartopsychops* Badano & Engel, *Acanthopsychops* Badano & Engel (both Cretaceous) and *Propsychopsis* Krüger (Eocene) within Psychopsidae, as well as *Nymphavus* Badano, Engel & Wang (Cretaceous) and *Pronymphes* Krüger (Eocene) in Nymphidae. Similarly, we recovered the Cretaceous fossil *Cladofer* Badano, Engel & Wang as nested within a group including Ithonidae and Nymphidae under both approaches. Both methods also agreed upon reconstructing the Cretaceous fossils *Adelpholeon* Badano & Engel, *Burmitus* Badano, Engel & Wang, *Diodontognathus* Badano, Engel & Wang, *Electrocaptivus* Badano, Engel & Wang as stem-group to the Myrmeleontidae + Ascalaphidae clade. The position of the Cretaceous antlion *Pristinofossor* Badano & Engel instead appeared conflicting. The combined analysis recovered it as sister to all Myrmeleontidae, while EPA placed it as a crown-antlion.

Discussion

The unique shape and puzzling features of *Ankyloleon* reinvigorate the question of how far lacewings explored the multidimensional ecological spaces of the Mesozoic. These features are so unique that make these specimens enigmatic from both phylogenetic and behavioural point of view.

An unusual abdomen

Our analyses show that *Ankyloleon* is phylogenetically related to Myrmeleontiformia, although none of the extant and extinct representatives of this large and diverse group share such a highly derived abdomen. However, larvae of lacewings and allies are often provided with pygopods or anal prolegs (Snodgrass, 1935); that is, soft and deformable protuberances at the end of the abdomen (Fig. 5) that improve contact and attachment to the substrate through a complex combination of van der Waals forces, capillary forces and friction (Zurek *et al.*, 2015). Pygopods often contribute to locomotion by acting as pivot points or grasping structures. Aquatic larvae of dobsonflies

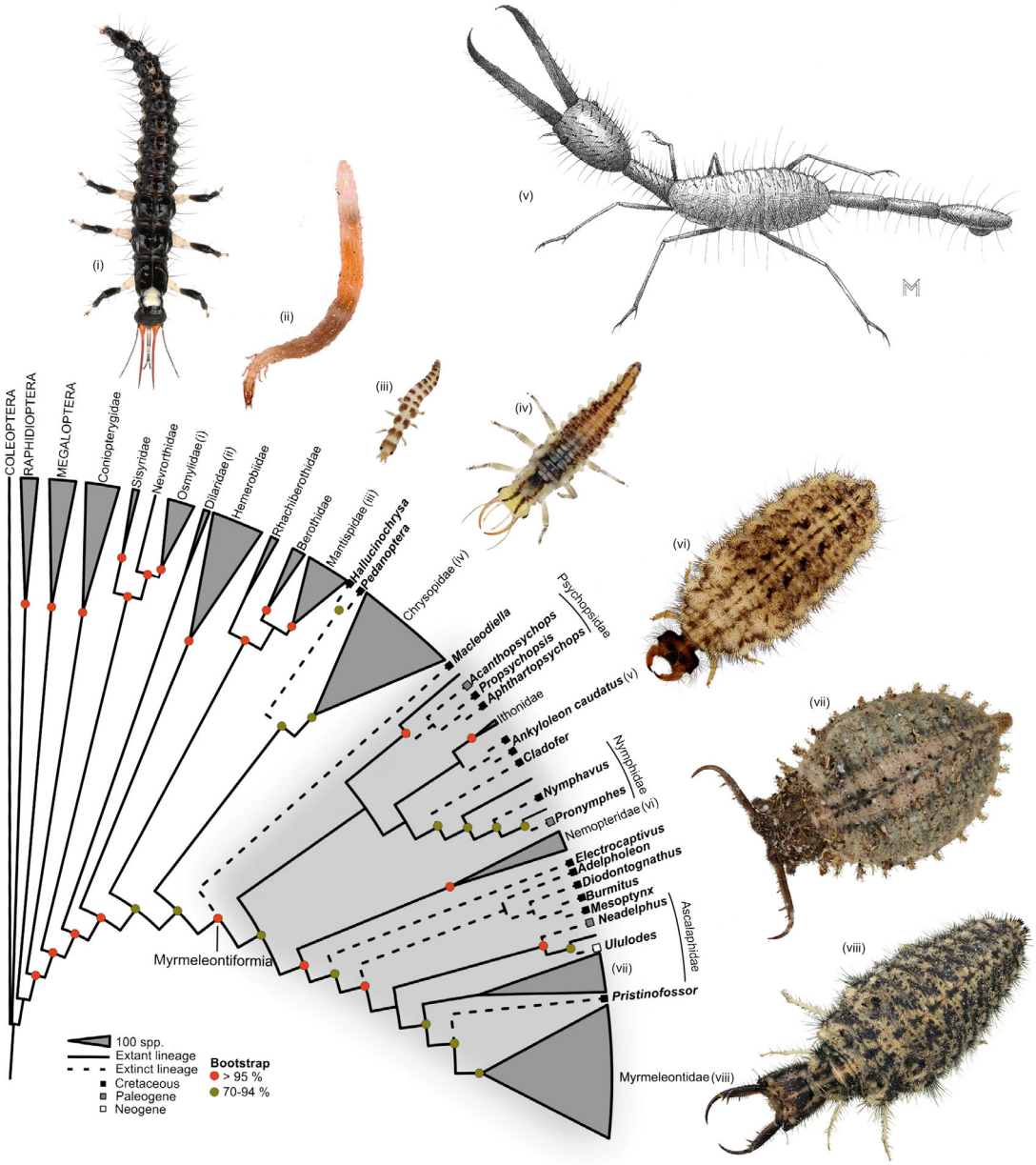

Fig. 4. Phylogeny of Neuroptera, highlighting the relationships of *Ankyloleon*. Based on the ML analysis of partitioned combined dataset including genomic and morphological data, see also Fig. S4. Fossil taxa are in bold characters. (i–vii) selected representatives of the diversity of lacewing larvae (not in scale): (i) Osmylidae larva indet. (photo by G. Montgomery); (ii) *Dilar* sp., Dilaridae; (iii) *Mantispa styriaca* (Poda), first instar, Mantispidae; (iv) *Chrysoperla mediterranea* Hölzel, Chrysopidae; (v) *Ankyloleon caudatus* **gen. et sp.n.** reconstruction; (vi) *Nemoptera bipennis* (Illiger) Nemopteridae; (vii) *Libelloides ictericus* (Charpentier) Ascalaphidae and (viii) *Brachynemurus ferox* (Walker), Myrmeleontidae. [Colour figure can be viewed at wileyonlinelibrary.com].

and fishflies (Megaloptera: Corydalidae), living in fast flowing rivers and creeks, evolved pygopods with terminal hooks or suckers to anchor themselves to the substrate. Conversely, terrestrial larvae of snakeflies (Raphidioptera) and of most lacewings–e.g., brown and green lacewings (Hemerobiidae and Chrysopidae), mantis flies (Mantispidae) and silky lacewings (Psychopsidae)–are provided with adhesive pygopods (Fig 5A, C–E). Lance lacewing larvae (Osmylidae), which might be terrestrial or amphibious, have paired soft, eversible structures with series of ventral hooks, forming a complex grasping apparatus (Fig. 5B). Finally, the larvae of antlions and owlflies (Myrmeleontidae) and thread- and spoon-winged lacewings (Nemopteridae) use abdominal segments 8 and 9 for digging and anchoring, usually by means of highly modified setae

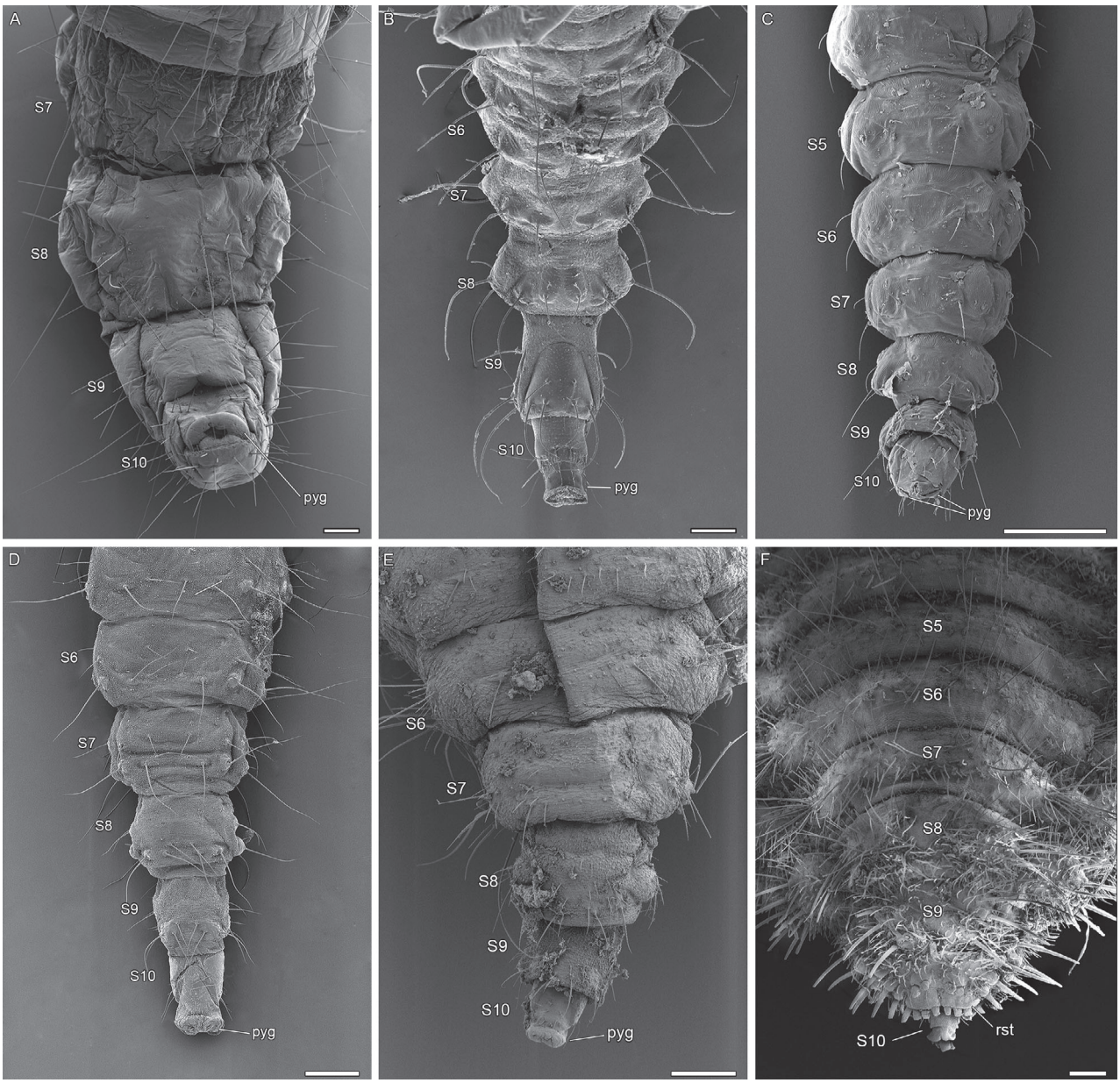

Fig. 5. Abdomen of lacewing larvae at scanning electron microscope. In ventral view: (A) *Phaeostigma* sp. (Raphidioptera: Raphidiidae); (B) *Osmylus fulvicephalus* Scopoli (Osmylidae); (C) *Mantispa styriaca* (Poda) (Mantispidae); (D) *Hemerobius* sp. (Hemerobiidae); (E) *Pseudomallada* sp. (Chrysopidae) and (F) *Euroleon nostras* Geoffroy *in* Fourcroy (Myrmeleontidae). Scale bar: 100 μm.

(Fig. 5F). Although no other lacewings share a similar morphology, beetles may offer insights into the role of this combination of features. Peculiar configurations of the tip of the abdomen in beetle larvae can be associated with predatory habits or with defensive purposes. The elongated abdominal segments 8–10 and the presence of apparently glandular structures on segment 10 would suggest that *Ankyloleon* was able to raise up and curve the 'tail' over the body, perhaps secreting repulsive or attractive/appeasing substances, as do several rove beetles (Coleoptera: Staphylinidae) and flanged bombardier beetles (Coleoptera: Carabidae, Paussinae) (Di Giulio & Vigna Taglianti, 2001; Parker, 2016). Texas beetle larvae (Coleoptera: Brachypsectridae), which resemble owlfly larvae in shape and behavior, instead use the spine-like abdomen tip to stab prey (Crowson, 1973; Costa *et al.*, 2006), suggesting that the abdomen of *Ankyloleon* might be potentially involved in predation, bringing the prey in contact with the mouthparts. The shape of abdominal segment 10 of *Ankyloleon* also recalls the condition of false flower beetle larvae (Coleoptera: Scraptiidae) (Švácha, 1995; Haug J.T. & Haug C., 2019). However, the caudal structure of scraptiids is accessory, as it can be shed off and then regenerated, whereas in *Ankyloleon*, segment 10 is

an integral part of the abdomen, as evidenced by the presence of vesicles (Figs 1B, 3B–F). XPCT reconstructions suggest that the ventral vesicles were pygopod-like structures, perhaps associated with glands as found in some beetles where pygopods produce adhesive substances (Zurek *et al.*, 2015) (Fig 3D–F). A secretive function is supported by the presence of a median duct and external pore (Fig 3C). A flexible abdomen, provided with prominent pygopods, might have proven useful to move on smooth surfaces, at the same time maintaining a grip through adhesive secretions. However, as often happens, a complex anatomical structure may have more than one role, as well as hidden functions that cannot be readily inferred from morphology without extant analogues.

What does the head say about the natural history of Ankyloleon*?*

As with bird beaks, jaws of lacewing larvae mirror alimentary specializations and life habits. Nearly all extant lacewing larvae (perhaps with few exceptions) are predators (Oswald & Machado, 2018) and *Ankyloleon*, being characterized by elongated, straight and apically hooked jaws was not an exception (Figs 1, 2, 3A). The articulation of the mandibular-maxillary stylets with the head shows that these larvae were not able to widely open their jaws as owlflies or antlions do in a trap-like fashion (Badano *et al.*, 2017). This seeming disadvantage was likely counterbalanced by a highly mobile head–thorax articulation and elongate prothorax (Figs 1, 2), like the extinct *Macleodiella* and extant nevrorthids and thread lacewing (Crocinae) larvae (Beutel *et al.*, 2010; Badano *et al.*, 2018). Sense organs of *Ankyloleon* can also provide information on its life history. Both eyes (stemmata) and antennae were reduced, whereas labial palps were absent, suggesting that visual and chemical stimuli were likely not relevant for these larvae (Figs 1, 2, 3A). *Ankyloleon* was equipped with a diverse array of trichoid sensilla, especially on the head and segment 10 (Fig. 1), suggesting these mechanoreceptors were the main sense organs, as in living antlions (Devetak *et al.*, 2007; Podlesnik *et al.*, 2019). The thin hair-like sensilla on the terminal club had likely a similar tactile function, allowing larvae to sense the surroundings and to navigate within dark and narrow spaces.

Palaeoecology

Arthropod assemblages preserved in Cenozoic ambers originating from angiosperms are known to be biased towards species living or climbing on the resin-producing trees (Solórzano Kraemer *et al.*, 2015, 2018). In contrast, it is still debated whether arthropod amber inclusions from the Mesozoic provide an accurate rendition of a whole forest insect paleofauna (Peris *et al.*, 2016). Nonetheless, bark dwelling neuropteroid larvae appear particularly well represented in Burmese amber, including snakeflies, silky lacewings and Myrmeleontiformia (Badano *et al.*, 2018; Haug G.T. *et al.*, 2020; Haug J.T. *et al.*, 2020), implying that most of them were entrapped in resin in situ. Phylogenetic and fossil evidence also suggest that the oldest representatives of Myrmeleontiformia were arboreal (Oswald & Machado, 2018; Badano *et al.*, 2018). All evidence hints at *Ankyloleon* as an arboreal thigmotactic predator, using the terminal abdominal segments 7–10 as a pivot point. The shape of head and jaws suggest that *Ankyloleon* struck prey from afar, probably tiny insects with soft cuticle.

Fossil phylogenetic signal

The inclusion of fossil taxa in phylogenetic reconstructions provides information on character polarity, trait evolution and valuable calibration points for clade divergence time estimations (Ware & Barden, 2016). Nevertheless, the phylogenetic relationships of fossil taxa are often hypothesized based on non-numerical, morphological approaches, which are only rarely tested using explicit, quantitative methods. In the case of lacewings, the long-lasting concept that larval morphology is generally a reliable indicator of higher-level phylogeny (Aspöck *et al.*, 2001; Badano *et al.*, 2017; Haug J.T. & Haug C., 2019) has been recently challenged by phylogenomic analyses, which highlighted that the evolution of morphological traits is likely more complex than predicted by cladistic methods (Winterton *et al.*, 2018; Vasilikopoulos *et al.*, 2020). Therefore, we integrated morphological and genomic data to make the phylogenetic placement of fossil taxa explicit and replicable. Our ML analysis of the combined dataset reconstructed the phylogenetic position of fossil taxa largely consistent with Badano *et al.* (2018) (Fig. 4). The main difference from the cladistic reconstruction of Badano et al. (2018) involves the affinities of *Cladofer*, which was not retrieved sister to *Macleodiella* (see also Figs S6, S7) but deeply nested within Myrmeleontiformia (Fig. 4). Moreover, EPA recovered *Hallucinochrysa* and *Pristinofossor* as crown-group Chrysopidae and Myrmeleontidae (Fig. S5), respectively, whereas the combined analysis agreed with Badano et al. (2018) by yielding *Hallucinochrysa* sister to *Pedanoptera* and *Pristinofossor* as a stem-group myrmeleontid (Figs 4, S4). The position of *Ankyloleon* varies according to the method employed. Despite these differing results, both approaches agreed in placing *Ankyloleon* within Myrmeleotiformia, even though this taxon does not share all the apomorphies supporting monophyly of the crown group. The state of preservation, the amount of available information and the unusual combination of characters likely account for the variable phylogenetic reconstructions of *Ankyloleon*. Myrmeleontiformia diverged from other Neuroptera in the Late Triassic, whereas the major subgroups diversified in the Jurassic or Early Cretaceous (Winterton *et al.*, 2018; Vasilikopoulos *et al.*, 2020). Our analyses confirm that all major extant lineages of Myrmeleontiformia were already present at the beginning of the Late Cretaceous and coexisted with stem-group relicts from the first diversification wave of the clade. The fossil placement also corroborates that early representatives of Myrmeleontiformia, including *Ankyloleon* and *Macleodiella*, were characterized by small-sized elongated larvae that likely lived in arboreal settings. Our results show that integrating morphological and molecular evidence permits the reconstruction of the

phylogenetic placement of extinct body organizations, enabling the testing of hypotheses about insect evolution.

Conclusions

The fossil record continues to deliver new information about insect evolution, revealing that our current understanding of their impressive diversity and disparity is largely distorted by extinction events. Fossils also show that the radiation of insects was much wider than present-day diversity would suggest. Our study supports the view that the inclusion of extinct forms into phylogenetic analysis often has a deep impact on the relationships among living organisms and is critical to our understanding of the origin of certain morphological and behavioural features (Mongiardino Koch & Parry, 2020). The picture rendered by phylogenetic trees including fossils suggests that extinction often acts as a tight sieve that only allows a few lineages through. In this evolutionary process, survivors further diversify, evolving new features that might eventually disappear in favour of new ones.

Supporting Information

Additional supporting information may be found online in the Supporting Information section at the end of the article.

Figure S1. *Ankyloleon* specimen 1 (MZURPAL00112), detail of the abdomen in dorsolateral view.

Figure S2. *Ankyloleon* specimen 3 (PED_0118): (A) dorsal view, (B) colour marked version, (C) detail of jaw and (D) micro-CT scan.

Figure S3. *Ankyloleon* specimen 4 (PED_0454): (A) dorsal view, (B) colour marked version and (C) detail of the head.

Figure S4. Phylogram of Neuroptera, including extinct and living taxa, based on the ML analysis of partitioned combined dataset including genomic and morphological data.

Figure S5. Placement of fossil lacewing larvae on the ML phylogram based on the Evolutionary Placement Algorithm implemented on RAxML.

Figure S6. Strict consensus cladogram obtained from 36 most parsimonious trees resulting from the maximum parsimony analysis of the morphological dataset under equal weights (tree length: 359; consistency index: 0.53; retention index: 0.88).

Figure S7. Shortest tree with highest total fit obtained from the maximum parsimony analysis of the morphological dataset with optimized character state changes. Black and white squares indicate unique and nonunique apomorphies, respectively.

File S1. Data matrix for phylogenetic analysis.

Movie S1. Side view 3D reconstruction of *Ankyloleon caudatus* holotype.

Movie S2. Dorsoventral view 3D reconstruction of the head of *Ankyloleon caudatus* holotype.

Acknowledgements

We acknowledge the Paul Scherrer Institut, Villigen, Switzerland, for provision of synchrotron radiation beamtime at the TOMCAT beamline X02DA of the Swiss Light Source and would like to thank Margie Olbinado for assistance. We thank James E. O'Hara (Canadian National Collection of Insects Agriculture and Agri-Food Canada) and Moreno Di Marco (Sapienza University of Rome) for the critical review of the manuscript. We acknowledge Andrea Basso (Istituto Zooprofilattico Sperimentale delle Venezie) for his suggestions on the analyses. We thank Graham Montgomery for his photograph of the osmylid larva. Finally, we thank two anonymous reviewers for helpful comments and valuable suggestions on the manuscript. Davide Badano was supported by a SAPIExcellence BE-FOR-ERC fellowship (Sapienza University of Rome), Project "Tempo and Mode of Lacewing Evolution". Joachim T. Haug was kindly funded by the Volkswagen Foundation via a Lichtenberg professorship. The study was supported by the German Research Foundation (DFG HA 6300/6-1). The authors declare no conflict of interest.

Author contributions

Davide Badano and Pierfilippo Cerretti conceived and designed the study. Joachim T. Haug, Thomas Weiterschan and Jürgen Velten provided the materials. Davide Badano, Pierfilippo Cerretti and Joachim T. Haug studied, photographed and described the material. Michela Fratini, Laura Maugeri, Francesca Palermo, Nicola Pieroni and Alessia Cedola performed the experiment using XPCT and designed digital reconstructions and animations. Andrea Di Giulio examined the materials at scanning electron microscope. Davide Badano and Pierfilippo Cerretti assembled the dataset and analysed the data. Maurizio Mei contributed to logistics and materials tools and made the line drawings. Davide Badano and Pierfilippo Cerretti wrote the paper and made the figures. All authors edited and checked the manuscript.

Data availability statement

The data that supports the findings of this study are available in the supplementary material of this article

References

Aspöck, U., Plant, J.D. & Nemeschkal, H.L. (2001) Cladistic analysis of Neuroptera and their systematic position within the Neuropterida (Insecta: Holometabola: Neuropterida: Neuroptera). *Systematic Entomology*, **26**, 73–86.

Badano, D., Aspöck, U., Aspöck, H. & Cerretti, P. (2017) Phylogeny of Myrmeleontiformia based on larval morphology (Neuropterida: Neuroptera). *Systematic Entomology*, **42**, 94–117.

Badano, D., Engel, M.S., Basso, A., Wang, B. & Cerretti, P. (2018) Diverse Cretaceous larvae reveal the evolutionary and behavioural history of antlions and lacewings. *Nature Communications*, **9**, 1–14 https://doi.org/10.1038/s41467-018-05484-y.

Berger, S.A. & Stamatakis, A. (2010) Accuracy of morphology-based phylogenetic fossil placement under maximum likelihood. *Proceedings of IEEE/ACS International Conference on Computer Systems and Applications (AICCSA-10)*. IEEE Computer Society, Hammamet, Tunisia. 1–9. https://doi.org/10.1109/AICCSA.2010.5586939.

Berger, S.A., Stamatakis, A. & Lücking, R. (2011) Morphology-based phylogenetic binning of the lichen genera Graphis and Allographa (Ascomycota: Graphidaceae) using molecular site weight calibration. *Taxon*, **60**, 1450–1457.

Beutel, R.G., Friedrich, F. & Aspöck, U. (2010) The larval head of Nevrorthidae and the phylogeny of Neuroptera (Insecta). *Zoological Journal of the Linnean Society*, **158**, 533–562.

Beutel, R.G., Friedrich, F., Ge, S. & Yang, X. (2014) *Insect Morphology and Phylogeny*. De Gruyter, Berlin.

Bidola, P., Stockmar, M., Achterhold, K. *et al.* (2015) Absorption and phase contrast x-ray imaging in paleontology using laboratory and synchrotron sources. *Microscopy and Microanalysis*, **21**, 1288–1295.

Chernomor, O., von Haeseler, A. & Minh, B.Q. (2016) Terrace aware data structure for phylogenomic inference from supermatrices. *Systematic Biology*, **65**, 997–1008.

Costa, C., Vanin, S.A., Lawrence, J.F., Ide, S. & Branham, M.A. (2006) Review of the family Brachypsectridae (Coleoptera: Elateroidea). *Annals of the Entomological Society of America*, **99**, 409–432.

Crowson, R.A. (1973) On a new Superfamily Artematopoidea of polyphagan beetles, with the definition of two new fossil genera from the Baltic Amber. *Journal of Natural History*, **7**, 225–238.

Devetak, D., Mencinger-Vračko, B., Devetak, M., Marhl, M. & Špernjak, A. (2007) Sand as a medium for transmission of vibratory signals of prey in antlions *Euroleon nostras* (Neuroptera: Myrmeleontidae). *Physiological Entomology*, **32**, 268–274.

Di Giulio, A. & Vigna Taglianti, A. (2001) Biological observation on *Pachyteles* larvae (Coleoptera Carabidae Paussinae). *Tropical Zoology*, **14**, 157–173.

Engel, M.S., Winterton, S.L. & Breitkreuz, L.C.V. (2018) Phylogeny and evolution of Neuropterida: where have wings of lace taken us? *Annual Review of Entomology*, **63**, 531–551.

Goloboff, P.A. & Catalano, S.A. (2016) TNT version 1.5, including a full implementation of phylogenetic morphometrics. *Cladistics*, **32**, 221–238.

Grimaldi, D.A. & Engel, M.S. (2005) *Evolution of the Insects*. Cambridge University Press, Cambridge.

Haug, C., Herrera-Flórez, A.F., Müller, P. & Haug, J.T. (2019) Cretaceous chimera–an unusual 100-million-year old neuropteran larva from the "experimental phase" of insect evolution. *Palaeodiversity*, **12**, 1–11. https://doi.org/10.18476/pale.v12.a1.

Haug, G.T., Haug, C., Pazinato, P.G. *et al.* (2020) The decline of silky lacewings and morphological diversity of long-nosed antlion larvae through time. *Palaeontologia Electronica*, **23**, a39 (2020). https://doi.org/10.26879/1029.

Haug, J.T. & Haug, C. (2019) Beetle larvae with unusually large terminal ends and a fossil that beats them all (Scraptiidae, Coleoptera). *PeerJ*, **7**, e7871. https://doi.org/10.7717/peerj.7871.

Haug, J.T., Labandeira, C.C., Santiago-Blay, J.A., Haug, C. & Brown, S. (2015) Life habits, hox genes, and affinities of a 311 million-year-old holometabolan larva. *BMC Evolutionary Biology*, **15**, 208. https://doi.org/10.1186/s12862-015-0428-8.

Haug, J.T., Müller, P. & Haug, C. (2018) The ride of the parasite: a 100-million-year old mantis lacewing larva captured while mounting its spider host. *Zoological Letters*, **4**, 31. https://doi.org/10.1186/s40851-018-0116-9.

Haug, J.T., Müller, P. & Haug, C. (2019a) A 100-million-year old predator: a fossil neuropteran larva with unusually elongated mouthparts. *Zoological Letters*, **5**, 29. https://doi.org/10.1186/s40851-019-0144-0.

Haug, J.T., Müller, P. & Haug, C. (2019b) A 100-million-year old slim insectan predator with massive venom-injecting stylets – a new type of neuropteran larva from Burmese amber. *Bulletin of Geosciences*, **94**, 431–440. https://doi.org/10.3140/bull.geosci.1753.

Haug, J.T., Müller, P. & Haug, C. (2020) A 100 million-year-old snake-fly larva with an unusually large antenna. *Bulletin of Geosciences*, **95**, 167–177.

Hoang, D.T., Chernomor, O., von Haeseler, A., Minh, B.Q. & Vinh, L.S. (2018) UFBoot2: Improving the ultrafast bootstrap approximation. *Molecular Biology and Evolution*, **35**, 518–522. https://doi.org/10.1093/molbev/msx281.

Jandausch, K., Beutel, R.G. & Bellstedt, R. (2019) The larval morphology of the spongefly *Sisyra nigra* (Retzius, 1783) (Neuroptera: Sisyridae). *Journal of Morphology*, **280**, 1742–1758.

Kalyaanamoorthy, S., Minh, B.Q., Wong, T.K.F., von Haeseler, A. & Jermiin, L.S. (2017) ModelFinder: Fast model selection for accurate phylogenetic estimates. *Nature Methods*, **14**, 587–589.

Labandeira, C.C. (2018) The fossil history of insect diversity. *Insect Biodiversity: Science and Society, Vol. 2*, 2nd edn (ed. by R.G. Foottit and P.H. Adler), pp. 723–788. John Wiley & Sons Ltd., Oxford.

Lak, M., Néraudeau, D., Nel, A., Cloetens, P., Perrichot, V. & Tafforeau, P. (2008) Phase contrast X-ray synchrotron imaging: opening access to fossil inclusions in opaque amber. *Microscopy and Microanalysis*, **14**(25), 1–259.

Liu, X., Gongle, S., Fangyuan, X., Lu, X., Wang, B. & Engel, M.S. (2018) Liverwort mimesis in a Cretaceous lacewing larva. *Current Biology*, **28**, 1475–1481.

Liu, X., Zhang, W., Winterton, S.L., Breitkreuz, L.C.V. & Engel, M.S. (2016) Early morphological specialization for insect-spider associations in Mesozoic lacewings. *Current Biology*, **26**, 1590–1594.

Lu, X. & Liu, X. (2021) The Neuropterida from the mid-cretaceous of Myanmar: a spectacular palaeodiversity bridging the Mesozoic and present faunas. *Cretaceous Research*, **121**, 104727. https://doi.org/10.1016/j.cretres.2020.104727.

Miller, M.A., Pfeiffer, W.T. & Schwartz, T. (2010) Creating the CIPRES Science Gateway for inference of large phylogenetic trees. *Proceedings of the Gateway Computing Environments Workshop (GCE)*. New Orleans, 14 November 2010, pp. 1–8. https://doi.org/10.1109/GCE.2010.5676129

Minh, B.Q., Schmidt, H.A., Chernomor, O., Schrempf, D., Woodhams, M.D., von Haeseler, A. & Lanfear, R. (2020) IQ-TREE 2: New models and efficient methods for phylogenetic inference in the genomic era. *Molecular Biology and Evolution*, **37**, 1530–1534.

Misof, B., Liu, S.-L., Meusemann, K. *et al.* (2014) Phylogenomics resolves the timing and pattern of insect evolution. *Science*, **346**, 763–767.

Mongiardino Koch, N. & Parry, L.A. (2020) Death is on our side: paleontological data drastically modify phylogenetic hypotheses. *Systematic Biology*, **69**, 1052–1067. https://doi.org/10.1093/sysbio/syaa023.

Montagna, M., Tong, K.J., Magoga, G., Strada, L., Tintori, A., Ho, S.Y.W. & Lo, N. (2019) Recalibration of the insect evolutionary time scale using Monte San Giorgio fossils suggests survival of key lineages through the End-Permian Extinction. *Proceedings of the Royal Society B.*, **286**, 20191854 http://doi.org/10.1098/rspb.2019.1854.

Nel, A., Roques, P., Nel, P. *et al.* (2013) The earliest known holometabolous insects. *Nature*, **503**, 257–261.

Nixon, K.C. (2002) *Winclada, Version 1.00.08*. Published by the Author, Ithaca, New York. [WWW document]. URL http://www.cladistics.com. [accessed on 10 April 2015].

Oswald, J.D. & Machado, R.J.P. (2018) Biodiversity of the Neuropterida (Insecta: Neuroptera: Megaloptera, and Raphidioptera). *Insect Biodiversity: Science and Society, 2nd edn, Vol. 2* (ed. by R.G. Foottit and P.H. Adler), pp. 627–671. John Wiley & Sons Ltd., Oxford.

Parker, J. (2016) Myrmecophily in beetles (Coleoptera): evolutionary patterns and biological mechanisms. *Myrmecological News*, **22**, 65–108.

Pérez de la Fuente, R., Delclòs, X., Peñalver, E. & Engel, M.S. (2016) A defensive behavior and plant-insect interaction in Early Cretaceous amber – the case of the immature lacewing *Hallucinochrysa diogenesi*. *Arthropod Structure & Development*, **45**, 133–139.

Pérez de la Fuente, R., Delclòs, X., Peñalver, E., Speranza, M., Wierzchos, J., Ascaso, C. & Engel, M.S. (2012) Early evolution and ecology of camouflage in insects. *PNAS*, **109**, 21414–21419.

Pérez de la Fuente, R., Engel, M.S., Azar, D. & Peñalver, E. (2018a) The hatching mechanism of 130-million-year-old insects: an association of neonates, egg shells and egg bursters in Lebanese amber. *Palaeontology*, **62**, 547–559.

Pérez de la Fuente, R., Engel, M.S., Delclòs, X. & Peñalver, E. (2020) Straight-jawed lacewing larvae (Neuroptera) from lower Cretaceous Spanish amber, with an account on the known amber diversity of neuropterid immatures. *Cretaceous Research*, **106**, 104200 https://doi.org/10.1016/j.cretres.2019.104200.

Pérez de la Fuente, R., Peñalver, E., Azar, D. & Engel, M.S. (2018b) A soil-carrying lacewing larva in Early Cretaceous Lebanese amber. *Scientific Reports*, **8**, 1–12 https://doi.org/10.1038/s41598-018-34870-1.

Peris, D., Ruzzier, E., Perrichot, V. & Delclòs, X. (2016) Evolutionary and paleobiological implications of Coleoptera (Insecta) from Tethyan-influenced Cretaceous ambers. *Geosciences Frontiers*, **7**, 695–706.

Perreau, M. & Tafforeau, P. (2011) Virtual dissection using phase-contrast X-ray synchrotron microtomography: reducing the gap between fossils and extant species. *Systematic Entomology*, **36**, 573–580.

Peters, R.S., Meusemann, K., Petersen, M. *et al.* (2014) The evolutionary history of holometabolous insects inferred from transcriptome-based phylogeny and comprehensive morphological data. *BMC Evolutionary Biology*, **14**, 52. https://doi.org/10.1186/1471-2148-14-52.

Podlesnik, J., Klokočovnik, V., Lorent, V. & Devetak, D. (2019) Prey detection in antlions: propagation of vibrational signals deep into the sand. *Physiological Entomology*, **44**, 215–221.

Rainford, J.L., Hofreiter, M., Nicholson, D.B. & Mayhew, P.J. (2014) Phylogenetic distribution of extant richness suggests metamorphosis is a key innovation driving diversification in insects. *PLoS One*, **9**, e109085. https://doi.org/10.1371/journal.pone.0109085.

Rolff, J., Johnston, P.R. & Reynolds, S. (2019) Complete metamorphosis of insects. *Philosophical Transactions of the Royal Society B*, **374**, 20190063. https://doi.org/10.1098/rstb.2019.0063.

Shi, G., Grimaldi, D.A., Harlow, G.E. *et al.* (2012) Age constraint on Burmese amber based on U–Pb dating of zircons. *Cretaceous Research*, **37**, 155–163.

Snodgrass, R.E. (1935) *The Principles of Insect Morphology*. McGraw-Hill Book Company, New York, New York.

Solórzano Kraemer, M.M., Delclòs, X., Clapham, M.E. *et al.* (2018) Arthropods in modern resins reveal if amber accurately recorded forest arthropod communities. *PNAS*, **115**, 6739–6744.

Solórzano Kraemer, M.M., Kraemer, A.S., Stebner, F., Bickel, D.J. & Rust, J. (2015) Entrapment bias of arthropods in miocene amber revealed by trapping experiments in a Tropical Forest in Chiapas, Mexico. *PLoS ONE*, **10**, e0118820. https://doi.org/10.1371/journal.pone.0118820.

Soriano, C., Archer, M., Azar, D. *et al.* (2010) Synchrotron X-ray imaging of inclusions in amber. *Comptes Rendues Palevol*, **9**, 361–368.

Stamatakis, A. (2014) RAxML version 8: a tool for phylogenetic analysis and post-analysis of large phylogenies. *Bioinformatics*, **30**, 1312–1313.

Švácha, P. (1995) The larva of *Scraptia fuscula* (P.W.J. Müller) (Coleoptera: Scraptiidae): autotomy and regeneration of the caudal appendage. *Biology, Phylogeny, and Classification of Coleoptera: Papers Celebrating the 80th Birthday of Roy A. Crowson* (ed. by J. Pakaluk and S.A. Ślipiński), pp. 473–489. Muzeum i Instytut Zoologii, Varsavia.

Tafforeau, P., Boistel, R., Boller, E. *et al.* (2006) Applications of X-ray synchrotron microtomography for non-destructive 3D studies of paleontological specimens. *Applied Physics A*, **83**, 195–202.

Truman, J.W. (2019) The evolution of insect metamorphosis. *Current Biology*, **29**, R1252–R1258. https://doi.org/10.1016/j.cub.2019.10.009.

Truman, J.W. & Riddiford, L.M. (1999) The origins of insect metamorphosis. *Nature*, **401**, 447–452.

Vasilikopoulos, A., Misof, B., Meusemann, K. *et al.* (2020) An integrative phylogenomic approach to elucidate the evolutionary history and divergence times of Neuropterida (Insecta: Holometabola). *BMC Evolutionary Biology*, **20**, 64. https://doi.org/10.1186/s12862-020-01631-6.

Wang, B., Xia, F.Y., Engel, M.S. *et al.* (2016) Debris-carrying camouflage among diverse lineages of Cretaceous insects. *Sciences Advances*, **2**, 6. https://doi.org/10.1126/sciadv.1501918.

Ware, J.L. & Barden, P. (2016) Incorporating fossils into hypotheses of insect phylogeny. *Current Opinion in Insect Science*, **18**, 69–76.

Winterton, S.L., Lemmon, A.R., Gillung, J.P. *et al.* (2018) Evolution of lacewings and allied orders using anchored phylogenomics (Neuroptera, Megaloptera, Raphidioptera). *Systematic Entomology*, **43**, 330–354.

Yang, A.S. (2001) Modularity, evolvability, and adaptive radiations: a comparison of the hemi- and holometabolous insects. *Evolution & Development*, **3**, 59–72.

Zheng, D., Chang, S., Perrichot, V. *et al.* (2018) A late Cretaceous amber biota from central Myanmar. *Nature Communications*, **9**, 3170. https://doi.org/10.1038/s41467-018-05650-2.

Zurek, D.B., Gorb, S.N. & Voigt, D. (2015) Locomotion and attachment of leaf beetle larvae *Gastrophysa viridula* (Coleoptera, Chrysomelidae). *Interface Focus*, **5**, 20140055. https://doi.org/10.1098/rsfs.2014.0055.

Accepted 15 March 2021